A semi-continuous extended kinetic model for bimolecular chemical reactions

2000 J. Phys. A: Math. Gen. 33 6081

(http://iopscience.iop.org/0305-4470/33/35/302)

J. Phys. A: Math. Gen. **33** (2000) 6081–6094. Printed in the UK PII: S0305-4470(00)14450-6

A semi-continuous extended kinetic model for bimolecular chemical reactions

Winfried Koller

Institut für Theoretische Physik, Technische Universität Graz, Austria

Received 31 May 2000

Abstract. A semi-continuous kinetic approach to a four-component gas mixture undergoing elastic collisions as well as bimolecular chemical reactions is presented. General mass ratios of the four species are allowed for. Conservation laws as well as an H-theorem are established. Numerical solutions to simple spatially homogeneous test cases are provided.

1. Introduction

In the study of chemical reactions, gas kinetic approaches based on Boltzmann-like equations [1] have a long tradition. First investigations in this field were made by Prigogine and co-workers [2], who considered the Boltzmann equation for a dilute gas undergoing the reaction $A + A \rightarrow$ products. The appropriate microreversibility conditions linking endothermic and exothermic cross sections have been discussed in [3]. In [4], the Chapman–Enskog method was applied for the evaluation of chemical reaction rates. Later on, Grad's method was used [5] for the calculation of reaction rates and transport coefficients. A short summary of the development up to 1990 can be found in [6]. Quite recently, however, a rigorous H-theorem for the kinetic equations describing the evolution of the reacting gas mixture has been derived in [7] and [8]. The formalism of the latter work includes, in addition, internal energy levels of the gas particles as well as the interaction with a photon field.

This paper presents a discretization of the model analysed by Rossani and Spiga [7]. By generalizing the approach of Preziosi and Longo [9], semi-continuous kinetic equations for a mixture of four chemically reacting gases are provided and investigated. From a technical point of view, the major new aspect as compared to the model presented in [10] is the introduction of different masses of the involved species. This complicates the expressions for the conservation of momentum and energy. For this reason, discrete velocity models [11] for chemically reacting gas mixtures have not yet been established. In semi-continuous models, only the speed variable is discretized. This yields a higher flexibility of the scheme and allows one to deal with arbitrary mass ratios. To this end, it is necessary to generalize the original discretization procedure [9] by introducing a separate set of allowed speeds for each species.

The major advantage of the semi-continuous kinetic equations as compared to the scalar formulation of the Boltzmann equation [12, 13] resides in the capability of the former to treat spatially dependent problems. This can be done by expanding the distribution functions in terms of spherical harmonics [14].

0305-4470/00/356081+14$30.00

The paper is organized as follows. After stating the continuous kinetic equations in section 2, the semi-continuous kinetic model is established in section 3. The semi-continuous conservation laws as well as an H-theorem are discussed. In section 4, the spatially homogeneous equations are provided by resorting to a P_0 approximation. Finally, in section 5 some numerical results on the evolution of the distribution functions under the impact of the chemical reaction are discussed.

In the rest of this paper, we will denote the four gas species by A, B, C and D, respectively, whereas the letters N and M can stand for all of the four species.

2. Continuous kinetic equations

The kinetic description of the four-component gas mixture is formulated in terms of the distribution functions $f^N(\boldsymbol{v}, \boldsymbol{x}, t)$ for each species $N = \mathrm{A}, \mathrm{B}, \mathrm{C}, \mathrm{D}$ depending on velocity $\boldsymbol{v}$, space $\boldsymbol{x}$ and time t. The evolution of the distribution functions is affected by elastic binary collisions ($N + M \rightleftharpoons N + M$) as well as chemical reactions

$$\mathrm{A} + \mathrm{B} \rightleftharpoons \mathrm{C} + \mathrm{D}. \tag{1}$$

During the reactions, kinetic energy is transferred to internal energy. Denoting the internal energy of N by E^N, the difference in internal energy due to stronger chemical bonds of C and D compared to A and B is given by $\Delta E = E^{\mathrm{C}} + E^{\mathrm{D}} - E^{\mathrm{A}} - E^{\mathrm{B}} > 0$.

After a polar decomposition of the momentum space [9], for any binary collision

$$N + M \rightleftharpoons N' + M' \tag{2}$$

the conservation of mass M, total energy E and momentum $\boldsymbol{R}$ can be written as

$$M = m + m_* = m' + m'_* \tag{3}$$

$$E = p^2/(2m) + p_*^2/(2m_*) = p'^2/(2m') + p_*'^2/(2m'_*) \pm \Delta E \tag{4}$$

$$\boldsymbol{R} = p\hat{\boldsymbol{\Omega}} + p_*\hat{\boldsymbol{\Omega}}_* = p'\hat{\boldsymbol{\Omega}}' + p'_*\hat{\boldsymbol{\Omega}}'_* \tag{5}$$

where m, m_*, m' and m'_* stand for the masses of N, M, N' and M', respectively. Equivalently, p, p_*, ... denote the moduli and $\hat{\boldsymbol{\Omega}}$, $\hat{\boldsymbol{\Omega}}_*$, ... the direction of the momenta. Primed symbols generally refer to post-collisional quantities.

The integro-differential equations [7] governing the evolution of the phase densities f^N are of the form

$$\frac{\partial f^N}{\partial t} + \boldsymbol{v} \cdot \frac{\partial f^N}{\partial \boldsymbol{x}} = \sum_{M=\mathrm{A},\mathrm{B},\mathrm{C},\mathrm{D}} J^{NM} + \mathcal{J}^N \tag{6}$$

where the term J^{NM} describes elastic binary collisions $N + M \rightleftharpoons N + M$ and $\mathcal{J}^N$ contains the impact of the chemical reaction on the evolution of species N. By decomposing the post-collisional relative velocity as $\boldsymbol{g}' = g'\hat{\boldsymbol{n}}'$, $|\hat{\boldsymbol{n}}'| = 1$, the elastic collision terms can be written as

$$J^{NM} = \int_{\mathbb{R}^3} \mathrm{d}\boldsymbol{v}_* \int_{\mathbb{S}^2} \mathrm{d}\hat{\boldsymbol{n}}'\, g\sigma^{NM}(g, \gamma)[f^N(\boldsymbol{v}')f^M(\boldsymbol{v}'_*) - f^N(\boldsymbol{v})f^M(\boldsymbol{v}_*)] \tag{7}$$

with the cross section σ^{NM} depending on the relative speed g and the cosine $\gamma = \cos\alpha = \hat{\boldsymbol{n}}\cdot\hat{\boldsymbol{n}}'$ of the angle of deflection α. The post-collisional velocities are given by

$$\boldsymbol{v}' = \frac{1}{M}(\boldsymbol{R} - gm^M\hat{\boldsymbol{n}}') \qquad \text{and} \qquad \boldsymbol{v}'_* = \frac{1}{M}(\boldsymbol{R} + gm^N\hat{\boldsymbol{n}}'). \tag{8}$$

For the reactive collisions, we introduce the speeds g_{NM} via $g_{NM}^2 = 2\Delta E/\mu^{NM}$, where $\mu^{NM} = m^N m^M/M$ represents the reduced mass. Then the relative speeds after a reactive collision read

$$g^- = \sqrt{\frac{\mu^{\mathrm{AB}}}{\mu^{\mathrm{CD}}}(g^2 - g_{\mathrm{AB}}^2)} \qquad \text{and} \qquad g^+ = \sqrt{\frac{\mu^{\mathrm{CD}}}{\mu^{\mathrm{AB}}}(g^2 + g_{\mathrm{CD}}^2)} \tag{9}$$

where g represents the relative speed before collision. The speed g^- refers to the endothermic ($\rightarrow$) and g^+ to the exothermic ($\leftarrow$) direction of the chemical reaction, respectively. Of course, $g' = g$ for elastic collisions. The terms accounting for reactive collisions (2) with the cross section $\sigma_{NM}^{N'M'}(g, \gamma)$ read

$$\mathcal{J}^N = \int_{\mathbb{R}^3} \mathrm{d}\boldsymbol{v}_* \int_{\mathbb{S}^2} \mathrm{d}\hat{\boldsymbol{n}}'\, g\sigma_{NM}^{N'M'}(g, \gamma) \left[\left(\frac{\mu^{NM}}{\mu^{N'M'}} \right)^3 f^{N'}(\boldsymbol{v}') f^{M'}(\boldsymbol{v}_*') - f^N(\boldsymbol{v}) f^M(\boldsymbol{v}_*) \right]. \tag{10}$$

Here, the gain terms result from microreversibility conditions [3] of the form

$$(\mu^{\mathrm{CD}})^2 g^2 \sigma_{\mathrm{CD}}^{\mathrm{AB}}(g, \gamma) = (\mu^{\mathrm{AB}})^2 (g^+)^2 \sigma_{\mathrm{AB}}^{\mathrm{CD}}(g^+, \gamma). \tag{11}$$

The post-collisional velocities depending on the relative speed after collision $g' = g^-$ for $N = \mathrm{A}, \mathrm{B}$ and $g' = g^+$ for $N = \mathrm{C}, \mathrm{D}$ are given by

$$\boldsymbol{v}' = \frac{1}{M}(\boldsymbol{R} - m^{M'} g' \hat{\boldsymbol{n}}') \qquad \boldsymbol{v}_*' = \frac{1}{M}(\boldsymbol{R} + m^{N'} g' \hat{\boldsymbol{n}}'). \tag{12}$$

The conservation of mass, momentum and total energy as well as an H-theorem for the above sketched model are derived in [7]. Moreover, Maxwellians are found as equilibrium solutions, and in chemical equilibrium the mass action law is recovered.

3. Semi-continuous kinetic model

In order to discretize the kinetic equations of the previous section, we apply a generalized form of the procedure introduced in [9]. This strategy has already been adopted for the discretization of an extended kinetic model [10]. In principle, semi-continuous extended kinetic equations are derived by discretizing the speed variable in an appropriate manner.

Following these lines, we restrict the range of the particle's kinetic energies to the interval $I_v = [E_m, E_M)$, $0 < E_m < E_M < \infty$. All particles with kinetic energies outside I_v will be neglected. We introduce an arithmetical sequence of energies

$$E_i = E_m + (i + \tfrac{1}{2})\delta \qquad i = 0, 1, \ldots, n \tag{13}$$

with $\delta = (E_M - E_m)/(n + 1)$ being the centres of the subintervals (energy groups)

$$I_i = \left[E_i - \frac{\delta}{2}, E_i + \frac{\delta}{2} \right] \qquad i = 0, 1, \ldots, n. \tag{14}$$

Since we allow for different masses m^N, this results in different sets of speed knots

$$v_i^N = \sqrt{\frac{2}{m^N}\left(E_m + \left(i + \frac{1}{2} \right)\delta \right)} \tag{15}$$

for each species. The associated momenta are given by $p_i^N = m^N v_i^N$. Furthermore, we have to adapt the energy gap ΔE in such a way that it fits into the discretization scheme. Therefore we set $\Delta E = q\delta$ with $q \in \{1, 2, \ldots, 2n - 1\}$.

This form of discretization has the advantage of a simple expression for the conservation of energy. In fact, by labelling the energy groups of N, M, N', M' by i, j, h, k, respectively,

for elastic collisions, energy conservation is expressed by $i + j = h + k$. Moreover, also the reactive collisions imply $i + j = h + k \pm q$.

For the derivation of the collision terms of the semi-continuous model, we discuss the range of allowed solid angles in a collision process where the speeds are fixed. To this end, we consider the square of equation (5), i.e.

$$p^2 + p_*^2 + 2pp_*\hat{\boldsymbol{\Omega}} \cdot \hat{\boldsymbol{\Omega}}_* = p'^2 + p_*'^2 + 2p'p_*'\hat{\boldsymbol{\Omega}}' \cdot \hat{\boldsymbol{\Omega}}_*'. \tag{16}$$

As a consequence of $-1 \leqslant \hat{\boldsymbol{\Omega}}' \cdot \hat{\boldsymbol{\Omega}}_*' \leqslant 1$, the last formula implies the restriction

$$\frac{1}{2pp_*}((p' - p_*')^2 - p^2 - p_*^2) \leqslant \hat{\boldsymbol{\Omega}} \cdot \hat{\boldsymbol{\Omega}}_* \leqslant \frac{1}{2pp_*}((p' + p_*')^2 - p^2 - p_*^2). \tag{17}$$

For a fixed $\hat{\boldsymbol{\Omega}}$, the set of all $\hat{\boldsymbol{\Omega}}_*$ satisfying the above condition will be referred to as $D_*(p, p_*, p', p_*')$. Moreover, by differentiation of equation (16) and by following the lines of the proof of proposition 2.4 in [9], we obtain

$$\frac{\partial(\hat{\boldsymbol{\Omega}}', \hat{\boldsymbol{\Omega}}_*')}{\partial(\hat{\boldsymbol{\Omega}}, \hat{\boldsymbol{\Omega}}_*)} = \frac{\partial(\hat{\boldsymbol{\Omega}}' \cdot \hat{\boldsymbol{\Omega}}_*')}{\partial(\hat{\boldsymbol{\Omega}} \cdot \hat{\boldsymbol{\Omega}}_*)} = \frac{pp_*}{p'p_*'}. \tag{18}$$

This important relation is necessary to switch from integration over pre-collisional velocities to integration over post-collisional velocities in the collision terms [10].

Following [9], we express the unit vector of the post-collisional relative speed $\hat{\boldsymbol{n}}'$ in an appropriate frame of reference $(\hat{\boldsymbol{R}}, \hat{\boldsymbol{e}}_{\boldsymbol{R}}, \hat{\boldsymbol{e}}_\perp)$ as

$$\hat{\boldsymbol{n}}' = \cos\varphi'\hat{\boldsymbol{R}} + \sin\varphi'(\cos\vartheta\,\hat{\boldsymbol{e}}_{\boldsymbol{R}} + \sin\vartheta\,\hat{\boldsymbol{e}}_\perp). \tag{19}$$

The angles φ' and ϑ denote the usual parameters in polar coordinates. The angle of deflection α and thus the post-collisional solid angles can be considered as functions of the variables $(v, v_*, v', \hat{\boldsymbol{\Omega}}, \hat{\boldsymbol{\Omega}}_*, \vartheta)$. These considerations imply that the surface element $\mathrm{d}\hat{\boldsymbol{n}}'$ appearing in the collision terms of the continuous equations can be written as

$$\mathrm{d}\hat{\boldsymbol{n}}' = -\,\mathrm{d}(\cos\varphi')\,\mathrm{d}\vartheta = \frac{M^2 v'}{m^{M'} g' R}\,\mathrm{d}v'\,\mathrm{d}\vartheta. \tag{20}$$

Moreover, in the elastic case we have $g' = g$, $N' = N$ and $M' = M$.

Now we introduce the set of distribution functions $\boldsymbol{f} = \{f_i^N(\hat{\boldsymbol{\Omega}}, \boldsymbol{x}, t) \equiv f^N(v_i^N\hat{\boldsymbol{\Omega}}, \boldsymbol{x}, t)\}$, $i = 0, \ldots, n$, $N = \mathrm{A}, \mathrm{B}, \mathrm{C}, \mathrm{D}$. The kinetic equations for the evolution of $\boldsymbol{f}$ are obtained by resorting to the discretization procedure of [9] and [10]. In principle, equation (6) is integrated over each energy group. When appearing as an integrand, any function of kinetic energy (and thus of speed v) is approximated by a piecewise constant interpolant defined over the above stated discretization. The resulting equations are of the form

$$\frac{\partial f_i^N}{\partial t} + v_i^N\hat{\boldsymbol{\Omega}} \cdot \frac{\partial f_i^N}{\partial \boldsymbol{x}} = \mathcal{J}_i^N + \sum_M J_i^{NM} \tag{21}$$

where J_i^{NM} denotes the influence of elastic collisions between species N and species M on the evolution of the ith energy group of species N. Similarly, $\mathcal{J}_i^N$ contains the impact of chemical reactions on the ith energy group of species N.

3.1. Elastic collisions

In analogy to the formulation given in [9] and [10], the elastic semi-continuous collision term for the collision $N + M \rightleftharpoons N + M$ reads

$$J_i^{NM}[f^N, f^M] = \frac{\delta^2}{m^M m^N}\sum_{j=0}^{n} v_j^M \sum_{\substack{h,k=0 \\ i+j=h+k}}^{n} \int_0^{2\pi}\mathrm{d}\vartheta \int_{D_*(m^N v_i^N, m^M v_j^M, m^N v_h^N, m^M v_k^M)} \mathrm{d}\hat{\boldsymbol{\Omega}}_*$$
$$\times\{A_{ij}^{hk}(\hat{\boldsymbol{\Omega}} \cdot \hat{\boldsymbol{\Omega}}_*, \vartheta)\}^{NM}[f_k^M(\hat{\boldsymbol{\Omega}}_*')f_h^N(\hat{\boldsymbol{\Omega}}') - f_j^M(\hat{\boldsymbol{\Omega}}_*)f_i^N(\hat{\boldsymbol{\Omega}})]. \tag{22}$$

In this case, the pre- and post-collisional solid angles are given by

$$\begin{aligned} \hat{\boldsymbol{\Omega}} &= \frac{1}{v_i^N M}(\boldsymbol{R} - m^M g\hat{\boldsymbol{n}}) \qquad & \hat{\boldsymbol{\Omega}}_* &= \frac{1}{v_j^M M}(\boldsymbol{R} + m^N g\hat{\boldsymbol{n}}) \\ \hat{\boldsymbol{\Omega}}' &= \frac{1}{v_h^N M}(\boldsymbol{R} - m^M g\hat{\boldsymbol{n}}') \qquad & \hat{\boldsymbol{\Omega}}'_* &= \frac{1}{v_k^M M}(\boldsymbol{R} + m^N g\hat{\boldsymbol{n}}'). \end{aligned} \tag{23}$$

By taking into account the expression for the surface element $\mathrm{d}\hat{\boldsymbol{n}}'$ as given in equation (20), we find for the kernel

$$\{A_{ij}^{hk}(\hat{\boldsymbol{\Omega}}\cdot\hat{\boldsymbol{\Omega}}_*, \vartheta)\}^{NM} = \frac{M^2}{m^M R}\sigma^{NM}(g, \vartheta). \tag{24}$$

As a consequence of the microreversibility of the cross section, i.e. $\sigma^{NM}(g, \gamma) = \sigma^{MN}(g, \gamma)$, this kernel displays the symmetry

$$m^M\{A_{ij}^{hk}(\hat{\boldsymbol{\Omega}}\cdot\hat{\boldsymbol{\Omega}}_*, \vartheta)\}^{NM} = m^N\{A_{ji}^{kh}(\hat{\boldsymbol{\Omega}}_*\cdot\hat{\boldsymbol{\Omega}}, \vartheta)\}^{MN} \tag{25}$$

if we exchange the role of N and M. Moreover, by substituting pre-collisional quantities for post-collisional ones without exchanging N and M, we obtain

$$\{A_{ij}^{hk}(\hat{\boldsymbol{\Omega}}\cdot\hat{\boldsymbol{\Omega}}_*, \vartheta)\}^{NM} = \{A_{hk}^{ij}(\hat{\boldsymbol{\Omega}}'\cdot\hat{\boldsymbol{\Omega}}'_*, \vartheta)\}^{NM}. \tag{26}$$

As usual, these expressions have to be combined with the Jacobian, i.e. equation (18), where, of course, for elastic collisions the masses cancel out.

3.2. Reactive collisions

In this subsection, the semi-continuous collision terms for the bimolecular chemical reaction (1) are presented. For brevity, we consider the general interaction stated in equation (2). The discretization yields

$$\begin{aligned} \mathcal{J}_i^N[\boldsymbol{f}] = \frac{\delta^2}{m^M m^{N'}}\sum_{j=0}^{n} v_j^M \sum_{\substack{h,k=0 \\ h+k=i+j\mp q}}^{n} \int_0^{2\pi}\mathrm{d}\vartheta \int_{D_*(m^N v_i^N, m^M v_j^M, m^{N'} v_h^{N'}, m^{M'} v_k^{M'})} \mathrm{d}\hat{\boldsymbol{\Omega}}_* \\ \times\{\mathcal{A}_{ij}^{hk}(\hat{\boldsymbol{\Omega}}\cdot\hat{\boldsymbol{\Omega}}_*, \vartheta)\}^N \left[\left(\frac{\mu^{NM}}{\mu^{N'M'}}\right)^3 f_k^{M'}(\hat{\boldsymbol{\Omega}}'_*) f_h^{N'}(\hat{\boldsymbol{\Omega}}') - f_j^M(\hat{\boldsymbol{\Omega}}_*) f_i^N(\hat{\boldsymbol{\Omega}})\right] \end{aligned} \tag{27}$$

where the minus sign in $\mp q$ applies for $N = \mathrm{A}, \mathrm{B}$ and the plus sign for $N = \mathrm{C}, \mathrm{D}$. Pre-collisional solid angles are the same as for elastic collisions whereas the post-collisional solid angles are given by

$$\hat{\boldsymbol{\Omega}}' = \frac{1}{v_h^{N'} M}(\boldsymbol{R} - m^{M'} g'\hat{\boldsymbol{n}}') \qquad \hat{\boldsymbol{\Omega}}'_* = \frac{1}{v_k^{M'} M}(\boldsymbol{R} + m^{N'} g'\hat{\boldsymbol{n}}'). \tag{28}$$

The kernels $\mathcal{A}$ are of the form

$$\{\mathcal{A}_{ij}^{hk}(\hat{\boldsymbol{\Omega}}\cdot\hat{\boldsymbol{\Omega}}_*, \vartheta)\}^N = \frac{gM^2}{g' R m^{M'}}\sigma_{NM}^{N'M'}(g, \vartheta) \tag{29}$$

with $g' = g^-$ for $N = \mathrm{A}, \mathrm{B}$ and $g' = g^+$ for $N = \mathrm{C}, \mathrm{D}$. The microreversibility conditions (11) and symmetry relations of the continuous kinetic description [7] imply

$$m^{M'}\{\mathcal{A}_{ij}^{hk}(\hat{\boldsymbol{\Omega}}\cdot\hat{\boldsymbol{\Omega}}_*, \vartheta)\}^N = m^{N'}\{\mathcal{A}_{ji}^{kh}(\hat{\boldsymbol{\Omega}}_*\cdot\hat{\boldsymbol{\Omega}}, \vartheta)\}^M \tag{30}$$

as well as

$$\frac{m^N m^M}{m^{N'}}\{\mathcal{A}_{ij}^{hk}(\hat{\boldsymbol{\Omega}}\cdot\hat{\boldsymbol{\Omega}}_*, \vartheta)\}^N = \frac{m^{N'} m^{M'}}{m^N}\{\mathcal{A}_{hk}^{ij}(\hat{\boldsymbol{\Omega}}'\cdot\hat{\boldsymbol{\Omega}}'_*, \vartheta)\}^{N'}. \tag{31}$$

3.3. Macroscopic quantities

In the semi-continuous formulation, the macroscopic quantities of each species N, namely the particle density, the mean velocity, the momentum flux and the kinetic energy flux, are respectively given by

$$n^N = \frac{\delta}{m^N} \sum_{j=0}^{n} v_j^N \int_{\mathbb{S}^2} f_j^N(\hat{\boldsymbol{\Omega}})\, \mathrm{d}\hat{\boldsymbol{\Omega}} \tag{32a}$$

$$\boldsymbol{u}^N = \frac{\delta}{m^N n^N} \sum_{j=0}^{n} (v_j^N)^2 \int_{\mathbb{S}^2} \hat{\boldsymbol{\Omega}} f_j^N(\hat{\boldsymbol{\Omega}})\, \mathrm{d}\hat{\boldsymbol{\Omega}} \tag{32b}$$

$$\mathbb{K}^N = \delta \sum_{j=0}^{n} (v_j^N)^3 \int_{\mathbb{S}^2} \hat{\boldsymbol{\Omega}} \otimes \hat{\boldsymbol{\Omega}} f_j^N(\hat{\boldsymbol{\Omega}})\, \mathrm{d}\hat{\boldsymbol{\Omega}} \tag{32c}$$

$$\boldsymbol{Q}^N = \frac{\delta}{2} \sum_{j=0}^{n} (v_j^N)^4 \int_{\mathbb{S}^2} \hat{\boldsymbol{\Omega}} f_j^N(\hat{\boldsymbol{\Omega}})\, \mathrm{d}\hat{\boldsymbol{\Omega}}. \tag{32d}$$

The kinetic energy density of species N is given by the trace $k^N = (\frac{1}{2})\,\mathrm{tr}\,\mathbb{K}^N$. The total energy density e of the gas mixture reads

$$e = \sum_M (k^M + n^M E^M). \tag{33}$$

We can now integrate the semi-continuous model equation (21) over all solid angles $\hat{\boldsymbol{\Omega}}$ and sum over all energy groups I_j. By using the definitions (32*a*)–(32*d*) and summing over all species, we obtain the macroscopic equations for the gas mixture,

$$\frac{\partial}{\partial t} \sum_M n^M + \frac{\partial}{\partial \boldsymbol{x}} \cdot \sum_M n^M \boldsymbol{u}^M = 0 \tag{34a}$$

$$\frac{\partial}{\partial t} \sum_M m^M n^M + \frac{\partial}{\partial \boldsymbol{x}} \cdot \sum_M m^M n^M \boldsymbol{u}^M = 0 \tag{34b}$$

$$\frac{\partial}{\partial t} \sum_M m^M n^M \boldsymbol{u}^M + \frac{\partial}{\partial \boldsymbol{x}} \cdot \sum_M \mathbb{K}^M = 0 \tag{34c}$$

$$\frac{\partial e}{\partial t} + \frac{\partial}{\partial \boldsymbol{x}} \cdot \sum_M \boldsymbol{Q}^M = 0 \tag{34d}$$

where the sums are extended over $M = \mathrm{A}, \mathrm{B}, \mathrm{C}$ and D. These equations reflect the conservation of particles, mass, total momentum, and total energy. As an impact of the chemical reactions, the individual densities n^N do not remain constant. Only their sum is preserved.

3.4. Properties of the collision terms

A proof of the conservation equations (34*a*)–(34*d*) involves symmetry properties of the collision terms. Therefore, adopting the notation of [10], for a set of arbitrary functions $\boldsymbol{\varphi} = \{\varphi_i^N(\hat{\boldsymbol{\Omega}}) \equiv \varphi^N(v_i^N \hat{\boldsymbol{\Omega}})\}$, $N = \mathrm{A}, \mathrm{B}, \mathrm{C}, \mathrm{D}$, $i = 0, \ldots, n$, we introduce

$$\langle \varphi^N, f^N \rangle = \frac{\delta}{m^N} \sum_{i=0}^{n} v_i^N \int_{\mathbb{S}^2} \mathrm{d}\hat{\boldsymbol{\Omega}}\, \varphi_i^N(\hat{\boldsymbol{\Omega}}) f_i^N(\hat{\boldsymbol{\Omega}}).$$

The main properties of the semi-continuous collision terms read as follows. First,

$$\langle\langle \boldsymbol{\varphi}, \boldsymbol{J} \rangle\rangle \equiv \sum_N \left\langle \varphi^N, \mathcal{J}^N + \sum_M J^{NM} \right\rangle \tag{35}$$

vanishes for $\varphi_i^N = 1; \varphi_i^N = m^N; \varphi_i^N = m^N v_i^N \hat{\boldsymbol{\Omega}}$ and $\varphi_i^N = m_i^N (v_i^N)^2/2 + E^N$. This correspond to the conservation equations stated in (34*a*)–(34*d*). Furthermore, we obtain a semi-continuous form of the space homogeneous H-theorem [7] by setting $\varphi_i^N = \log(f_i^N/(m^N)^3)$. It reads

$$\frac{\partial H}{\partial t} \equiv \langle\langle \log f, \boldsymbol{J} \rangle\rangle \leqslant 0. \tag{36}$$

This H-function is zero (collisional equilibrium of the gas mixture) if and only if

$$f_i^N(\hat{\boldsymbol{\Omega}}) = A^N \exp[m^N (v_i^N \boldsymbol{b} \cdot \hat{\boldsymbol{\Omega}} - c(v_i^N)^2)] \tag{37}$$

with the constants A^N, $\boldsymbol{b}$ and $c = 1/(2k_B T)$, where T is the common temperature of the mixture and k_B denotes Boltzmann's constant. The constants A^N are related via

$$\frac{A^C A^D}{A^A A^B} = \left(\frac{m^C m^D}{m^A m^B}\right)^3 \exp\left(-\frac{\Delta E}{k_B T}\right). \tag{38}$$

By inserting equation (37) with $\boldsymbol{b} = \boldsymbol{0}$ into equation (32*a*), we obtain in mechanical equilibrium

$$n^N = \frac{A^N}{(m^N)^{3/2}} \left\{ 4\pi\delta \sum_{j=0}^{n} \sqrt{2E_j} \mathrm{e}^{-E_j/k_B T} \right\} \tag{39}$$

which links the particle density n^N to the parameter A^N. The term in curly brackets is independent of N. Therefore, in chemical equilibrium we obtain from equation (38)

$$\frac{n^C n^D}{n^A n^B} = \left(\frac{m^C m^D}{m^A m^B}\right)^{3/2} \exp\left(-\frac{\Delta E}{k_B T}\right) \tag{40}$$

which is the mass action law [7].

A proof of these relations follows the lines of the proofs in section 4 of [10]. It applies the classical arguments of kinetic theory [1] by taking advantage of the Jacobian, i.e. equation (18). The microreversibility conditions, i.e. equations (25) and (26), are of crucial importance for the conservation properties of the elastic collision operators. More specifically, they imply $\langle 1, J^{NM} \rangle = 0$ as well as $\langle \varphi^N, J^{NM} \rangle + \langle \varphi^M, J^{MN} \rangle = 0$ for $\varphi_i^N = m^N v_i^N \hat{\boldsymbol{\Omega}}$ and $\varphi_i^N = m^N (v_i^N)^2/2$. Equivalently, equations (30) and (31) fulfill the same function for the collision operator relevant to chemical reactions. Moreover, they yield $\langle 1, \mathcal{J}^A \rangle = \langle 1, \mathcal{J}^B \rangle = -\langle 1, \mathcal{J}^C \rangle = -\langle 1, \mathcal{J}^D \rangle$.

4. Space homogeneous formulation

In this section, a first treatment of the solid angles $\hat{\boldsymbol{\Omega}}$ appearing in the semi-continuous model is presented. For simplicity, we confine ourselves to the case of a spatially homogeneous and isotropic chemically reacting gas mixture. Isotropic scattering will be assumed, which implies that the kernels A are independent of the angle ϑ. At this level we can study the evolution of the chemical reaction and the changes in the shape of the distribution functions of the gas mixture. Some illustrative numerical results are given in the subsequent section.

To derive the space homogeneous equations, we make the ansatz of the so-called P_0 approximation of the semi-continuous kinetic equations, i.e.

$$f_i^N(\hat{\boldsymbol{\Omega}}) = \frac{1}{4\pi v_i^N} n_i^N. \tag{41}$$

Apart from the multiplicative constant δ/m^N, the quantities

$$n_i^N = v_i^N \int_{\mathbb{S}^2} f_i^N(\hat{\boldsymbol{\Omega}}) \, \mathrm{d}\hat{\boldsymbol{\Omega}} \tag{42}$$

represent the number of particles N, $N = \mathrm{A}, \mathrm{B}, \mathrm{C}$ and D, within the energy group I_i. The evolution equations for the quantities n_i^N are obtained by integrating equation (21) with respect to $\hat{\boldsymbol{\Omega}}$:

$$\frac{\mathrm{d}n_i^N}{\mathrm{d}t} = \mathcal{Q}_i^N + \sum_M Q_i^{NM}. \tag{43}$$

This is a set of coupled ordinary differential equations. The integrated elastic collision terms read

$$Q_i^{NM} = \frac{\delta^2}{2m^N m^M} \sum_{j=0}^{n} \sum_{\substack{h,k=0 \\ h+k=i+j}}^{n} (\{I_{hk}^{ij}\}^{NM} n_h^N n_k^M - \{I_{ij}^{hk}\}^{NM} n_i^N n_j^M) \tag{44}$$

with the integrated elastic cross sections given by

$$\{I_{ij}^{hk}\}^{NM} = 2\pi \int_{u_0}^{u_1} \{A_{ij}^{hk}(u)\}^{NM}\, \mathrm{d}u = 2\pi \frac{M^2}{m^M} \int_{u_0}^{u_1} \frac{\sigma^{NM}(g)}{R}\, \mathrm{d}u. \tag{45}$$

Here,

$$g(u) = \sqrt{(v_i^{\mathrm{A}})^2 + (v_j^{\mathrm{B}})^2 - 2v_i^{\mathrm{A}} v_j^{\mathrm{B}} u} \qquad \text{and} \qquad R(u) = \sqrt{(p_i^{\mathrm{A}})^2 + (p_j^{\mathrm{B}})^2 + 2p_i^{\mathrm{A}} p_j^{\mathrm{B}} u}.$$

The domain of integration over $u = \hat{\boldsymbol{\Omega}} \cdot \hat{\boldsymbol{\Omega}}_*$, i.e. (u_0, u_1), coincides with the bound of the product $\hat{\boldsymbol{\Omega}} \cdot \hat{\boldsymbol{\Omega}}_*$ as given in equation (17). The symmetry and microreversibility conditions, i.e. equations (25) and (26), imply the relations

$$m^N \{I_{ji}^{kh}\}^{MN} = m^M \{I_{ij}^{hk}\}^{NM} \qquad \text{and} \qquad \{I_{hk}^{ij}\}^{NM} = \frac{v_h^N v_k^M}{v_i^N v_j^M} \{I_{ij}^{hk}\}^{NM}. \tag{46}$$

For hard spheres and Maxwell molecules, the elastic kernels I can be calculated analytically. The integrated collision term describing the influence of reactive interactions on species A is given by

$$\mathcal{Q}_i^{\mathrm{A}} = \frac{\delta^2}{2m^{\mathrm{B}} m^{\mathrm{C}} m^{\mathrm{D}}} \sum_{j=0}^{n} \sum_{\substack{h,k=0 \\ h+k=i+j-q}}^{n} \mathcal{K}_{ij}^{hk} \left(\tilde{\mu} \frac{v_i^{\mathrm{A}} v_j^{\mathrm{B}}}{v_h^{\mathrm{C}} v_k^{\mathrm{D}}} n_h^{\mathrm{C}} n_k^{\mathrm{D}} - n_i^{\mathrm{A}} n_j^{\mathrm{B}} \right). \tag{47}$$

For species B, the above formula applies with the substitutions $\mathrm{A} \leftrightarrow \mathrm{B}$, $\mathrm{C} \leftrightarrow \mathrm{D}$ and $\mathcal{K}_{ij}^{hk} \to \mathcal{K}_{ji}^{kh}$. A similar expressions can be found for the terms $\mathcal{Q}_i^{\mathrm{C}}$ and $\mathcal{Q}_i^{\mathrm{D}}$. In fact,

$$\mathcal{Q}_i^{\mathrm{C}} = \frac{\delta^2}{2m^{\mathrm{A}} m^{\mathrm{B}} m^{\mathrm{D}}} \sum_{j=0}^{n} \sum_{\substack{h,k=0 \\ h+k=i+j+q}}^{n} \mathcal{K}_{hk}^{ij} \left(n_h^{\mathrm{A}} n_k^{\mathrm{B}} - \tilde{\mu} \frac{v_h^{\mathrm{A}} v_k^{\mathrm{B}}}{v_i^{\mathrm{C}} v_j^{\mathrm{D}}} n_i^{\mathrm{C}} n_j^{\mathrm{D}} \right) \tag{48}$$

and, again, $\mathcal{Q}_i^{\mathrm{D}}$ is obtained by exchanging $\mathrm{A} \leftrightarrow \mathrm{B}$, $\mathrm{C} \leftrightarrow \mathrm{D}$ and $\mathcal{K}_{hk}^{ij} \to \mathcal{K}_{kh}^{ji}$. We have introduced $\tilde{\mu} = (\mu^{\mathrm{AB}}/\mu^{\mathrm{CD}})^3$. The quantities $\mathcal{K}$ are evaluated with the endothermic cross section

$$\mathcal{K}_{ij}^{hk} = 2\pi M^2 \int_{u_0}^{u_1} \frac{g}{g^- R} \sigma_{\mathrm{AB}}^{\mathrm{CD}}(g)\, \mathrm{d}u. \tag{49}$$

Microreversibility has been exploited to formulate these integrated collision terms.

5. Discussion of results

In this section, some results of the semi-continuous model are presented. They have been obtained by an implementation of the P_0 approximation sketched in the previous section. We discuss fast exothermic chemical reactions taking place in the mixture of hard-sphere particles of diameter $a = 3.46$ Å. The masses of the four species are chosen as $m^{\mathrm{A}} = 7$, $m^{\mathrm{B}} = 17$, $m^{\mathrm{C}} = 14$ and $m^{\mathrm{D}} = 10$ atomic mass units. The starting point of all calculations is mechanical (but not chemical) equilibrium of all four species at $T = 300$ K.

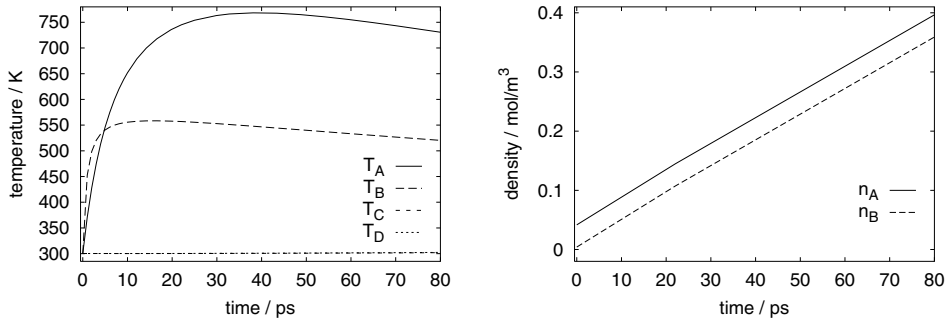

Figure 1. First few picoseconds of a fast highly exothermic chemical reaction. The left-hand plot shows the evolution of the temperatures and the right-hand plot the evolution of the densities of the products A and B. In the considered time interval, the densities of the reactants C and D remain virtually constant.

5.1. Simple exothermic reaction

We first study a chemical reaction described by the endothermic cross section $\sigma \sim \Theta(g - g^{\mathrm{AB}})g^{-}/g$, where $\Theta(\cdot)$ denotes the unit step function. For this choice, $\mathcal{K}$ can be calculated analytically. In fact, the integral in equation (49) is equivalent to that in (45) for hard spheres. The magnitude of the reactive cross section is chosen 60 times smaller than that for elastic interactions. The difference in internal energy is given by $\Delta E = 125$ meV. For the initial densities we choose

$$n^{\mathrm{A}} = 0.0416 \text{ mol m}^{-3} \qquad n^{\mathrm{B}} = 0.004\,16 \text{ mol m}^{-3}$$
$$n^{\mathrm{C}} = 4.16 \text{ mol m}^{-3} \qquad n^{\mathrm{D}} = 41.6 \text{ mol m}^{-3}.$$

Figure 1 shows the evolution of macroscopic quantities during the first 80 ps. Due to the initial rarity of species B, at the beginning the increase of particle number and temperature is most pronounced for this species. Here, temperature is understood as a measure for the mean kinetic energy per particle, i.e. $T^N = 2k^N/(3k_{\mathrm{B}}n^N)$. As can be seen in the right-hand plot of figure 1, the number of B particles is already 100 times greater at $t = 80$ ps than at the beginning.

During the considered period of time, the generated particles A and B undergo very few elastic collisions. Moreover, due to its smaller mass, A gains more kinetic energy from a reactive collision than B. This implies that the distribution function of A shows extreme deviations from a Maxwellian. Figure 2 illustrates this behaviour. On the other hand, the distribution functions of C and D stay virtually constant during the first 100 ps.

As the evolution continues, elastic collisions drive the gas towards mechanical equilibrium. For species A and B, this is sketched in figure 3. We see that after about 0.5 ns, all distributions functions have a strong resemblance to a Maxwellian although the generation of particles A and B has by far not finished yet. The distribution functions of species C and D are illustrated in figure 4. They only derive little from Maxwellians. The loss of particles C during the chemical reaction is considerable. On the scale of the left-hand plot of figure 4, the distribution function almost vanishes in the course of time. On the other hand, we observe only a little loss of species D as well as a shift of the maximum towards higher energies. This corresponds to the increasing temperature.

Figure 5 shows the evolution of the temperatures and densities of the various species for the first few nanoseconds of the evolution. We remark that the temperatures of the reactants C

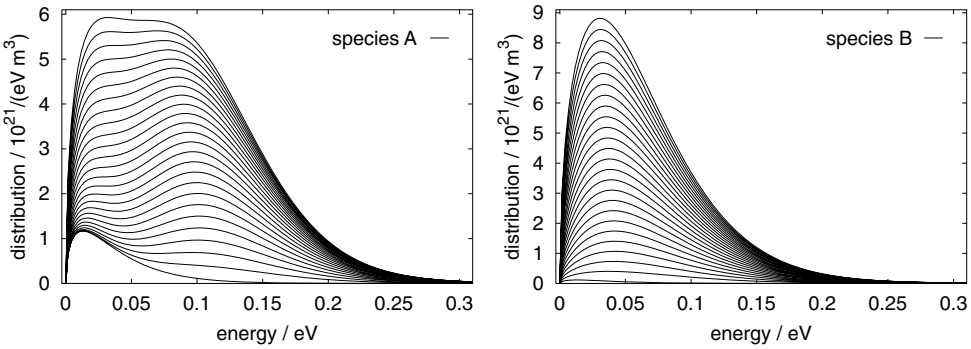

Figure 2. First few picoseconds of a fast highly exothermic chemical reaction. The plots shows the distribution functions of the products A and B at different instants of time after the ignition of the reaction. The lowest curves show the distribution at $t = 0$ whereas the highest curves correspond to $t = 125$ ps.

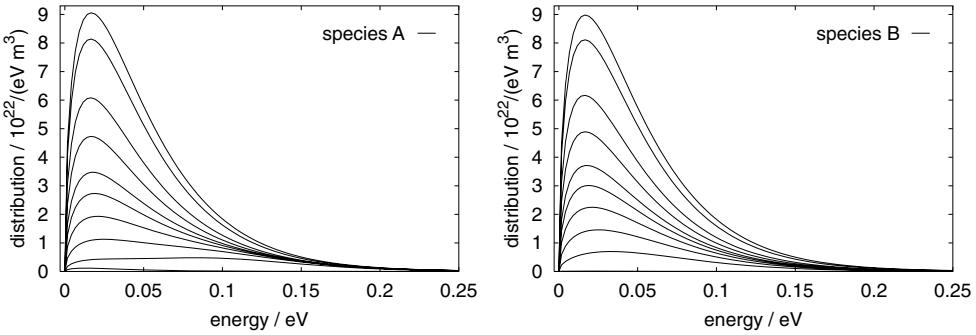

Figure 3. First 5 ns of a fast highly exothermic chemical reaction. Distribution functions of particles A and B at different instants of time after the ignition of the reaction. The highest curves correspond to $t = 5$ ns, followed by $t = 2$, 1, 0.7, 0.5, 0.4, 0.3, 0.2, 0.1 and 0 ns, respectively.

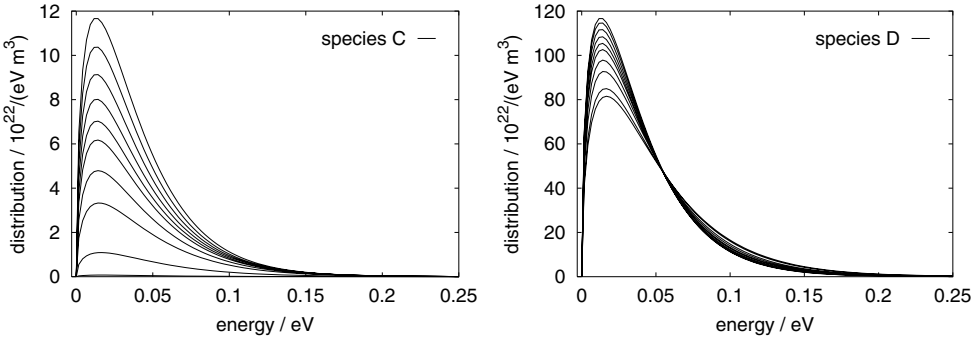

Figure 4. First 5 ns of a fast highly exothermic chemical reaction. Distribution functions of particles C and D at different instants of time after the ignition of the reaction. The maximum moves from the left (at $t = 0$) to the right (at $t = 5$ ns) and decreases in the course of time. The order of the curves is inverse to that given in figure 3.

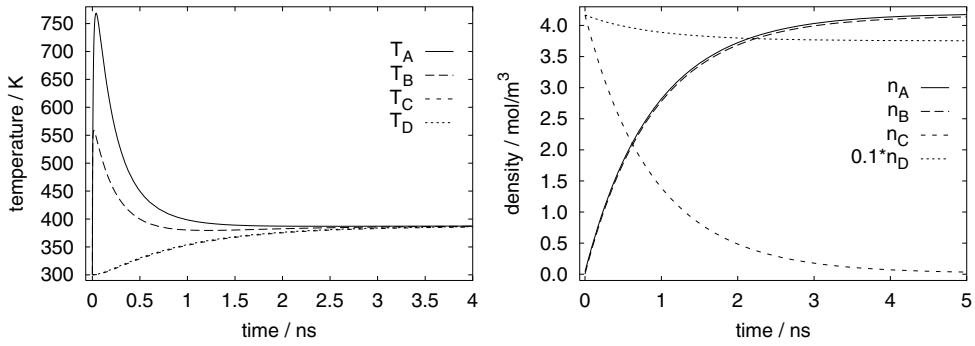

Figure 5. First few nanoseconds of a fast highly exothermic chemical reaction. The left-hand plot shows the evolution of temperature and the right-hand plot the evolution of the densities of the various gas species. For convenience, the density of species D is divided by ten.

and D increase to the common limit of about 387.48 K whereas those of the products A and B approach the limit from above. After 4 ns, a common temperature is reached and the four particle densities have almost arrived at constant levels. The final densities are given by

$$n^{\mathrm{A}} = 4.19 \text{ mol m}^{-3} \qquad n^{\mathrm{B}} = 4.16 \text{ mol m}^{-3}$$
$$n^{\mathrm{C}} = 0.0142 \text{ mol m}^{-3} \qquad n^{\mathrm{D}} = 37.51 \text{ mol m}^{-3}.$$

These values are in excellent agreement with the mass action law that predicts in equilibrium $n^{\mathrm{A}}n^{\mathrm{B}}/(n^{\mathrm{C}}n^{\mathrm{D}}) = 33.0$, which has to be compared with the actual value of 32.7 obtained from the numerical results. The discrepancy is less than 1%. It reflects the error the discretization introduces in the concept of temperature [9]. The temperature as a parameter of the Maxwellian (37) differs from the temperature as a measure for the mean kinetic energy per particle.

5.2. Exothermic threshold energy

Very interesting new features appear as soon as we introduce a threshold energy $r\delta$, $r \in \mathbb{N}$ for the exothermic direction of the chemical reaction. This can be done by means of the cross section described in [15], whose endothermic variant reads

$$\sigma_{\mathrm{AB}}^{\mathrm{CD}}(g) \sim \frac{1}{g^-}\left(1 - \frac{g_{\mathrm{AB}}^2 + g_x^2}{g^2}\right)\Theta(g^2 - (g_{\mathrm{AB}}^2 + g_x^2)). \tag{50}$$

The speed g_x is given by $g_x^2 = 2r\delta/\mu^{\mathrm{AB}}$. Due to this complicated structure, the integrals for the P_0 approximation are evaluated numerically. Since microreversibility has already been plugged into the P_0 equations, high accuracy is not needed because conservation laws are automatically satisfied.

The dynamics of the reaction depends critically on the threshold energy. According to its magnitude, we observe a more or less rapid ignition of the reaction.

Four cases are illustrated in figure 6, namely the case of a low, a medium, a high and a very high threshold. For the calculations, the distribution function is resolved using 76 energy groups. Measured in units of δ, the energy gap of the chemical reaction is given by $q = 50$ and the threshold by $r = 25$. The four different values for the threshold are obtained by modifying the width δ of the energy groups. We choose $\delta = 6.25$, 8.75, 11.25 and 12.5 meV, respectively.

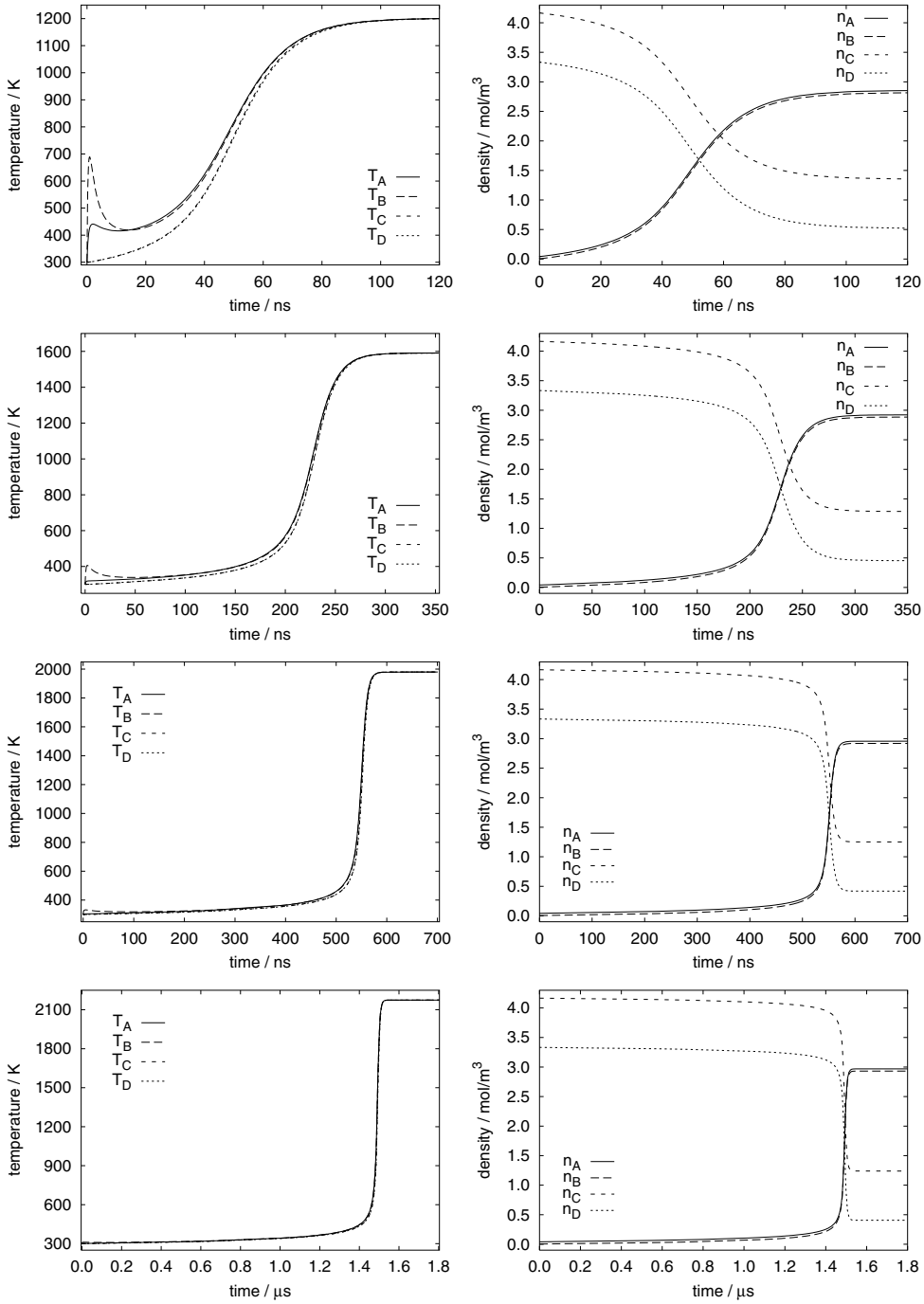

Figure 6. Evolution of temperatures and densities for a low (top), medium, high and very high (bottom) exothermic threshold energy.

The initial densities are given by

$$n^{\mathrm{A}} = 0.0416 \text{ mol m}^{-3} \qquad n^{\mathrm{B}} = 0.004\,16 \text{ mol m}^{-3}$$
$$n^{\mathrm{C}} = 4.16 \text{ mol m}^{-3} \qquad n^{\mathrm{D}} = 3.33 \text{ mol m}^{-3}.$$

For a low threshold energy, we first observe that the densities do not decay exponentially to their final values as in the case without exothermic threshold, cf figure 5. After an initial phase of about 20 ns where the temperatures of the products A and B go through a local maximum, they raise in concert with the temperatures of the reactants C and D. This accelerates the reaction. The pronounced peak of T^{B} is a consequence of the low initial density of B. Due to the conversion of internal energy to kinetic energy, the temperatures of A and B are always higher than those of C and D.

When the threshold is increased, the ignition becomes more and more delayed. At the beginning of the simulations, the gas mixture is cold. Consequently, few particles have sufficient kinetic energy to undergo a chemical reaction. These few reactions, however, constantly heat the gas mixture. An interesting aspect is that, at the beginning, the mean kinetic energy of the reactants decreases slightly (not visible in the plots). This is due to the fact that only the very energetic particles C and D react, being transformed to A and B. As soon as the temperature of C and D is high enough, ignition takes place followed by a rapidly increasing temperature. Obviously, for the highest value of the exothermic threshold energy, the ignition is delayed for the longest time.

6. Conclusion

In this paper, a semi-continuous extended kinetic model for a chemically reacting gas mixture is established. Four different species of gas undergoing elastic collisions as well as bimolecular chemical reactions are taken into account. General mass ratios of the involved species are allowed for.

The semi-continuous model reflects the major properties (H-theorem and conservation laws) of the full continuous kinetic description. Moreover, a mass action law governing the densities of the four species in chemical equilibrium is recovered.

The model is applied to calculate numerically the evolution of fast exothermic chemical reactions. At the level of the distribution functions, different degrees of deviation from Maxwellians due to fast reactive collisional processes are observed. In the studied case, the deviations are most obvious for the dominant species of the products.

A comparison of this model to a BGK model for chemical reactions is matter of current research activities. Spatially dependent simulations are scheduled as future work.

Acknowledgments

The author would like to express his gratitude towards the Rector of the Graz University of Technology for granting financial support. Various discussions with B Messnarz and F Schürrer have contributed to this paper. A pertinent remark from F Hanser is gratefully acknowledged.

References

[1] Cercignani C 1988 *The Boltzmann Equation and Its Applications* (New York: Springer)
[2] Prigogine I and Xhrouet E 1949 *Physica* **15** 913–32
[3] Light J C, Ross J and Shuler K E 1969 Rate coefficients, reaction cross sections and microscopic reversibility *Kinetic Processes in Gases and Plasmas* ed A R Hochstim (New York: Academic) 281ff

[4] Ross J and Mazur P 1961 *J. Chem. Phys.* **35** 19ff
[5] Moreau M 1975 *Physica* A **79** 18ff
[6] Boffi V C and Rossani A 1990 *J. Appl. Math. Phys. (ZAMP)* **41** 115–268
[7] Rossani A and Spiga G 1999 *Physica* A **272** 563–73
[8] Groppi M and Spiga G 1999 *J. Math. Chem.* **26** 197–219
[9] Preziosi L and Longo E 1997 *Japan. J. Indust. Appl. Math.* **14** 399–435
[10] Koller W, Hanser F and Schürrer F 2000 *J. Phys. A: Math. Gen.* **33** 3417–30
[11] Monaco R and Preziosi L 1991 *Fluid Dynamic Application of the Discrete Boltzmann Equation* (Singapore: World Scientific)
[12] Kügerl G and Schürrer F 1990 *Phys. Lett.* A **148** 158–63
[13] Kügerl G 1991 *J. Appl. Math. Phys. (ZAMP)* **42** 821–36
[14] Koller W and Schürrer F 2000 P_N approximation of the non-linear semi-discrete Boltzmann equation *Trans. Theor. Stat. Phys.* at press
[15] Griehsnig P, Schürrer F and Kügerl G 1994 *Rarefied Gas Dynamics: Theory and Application* ed B D Shizgal and D P Weaver (Oxford: Oxford University Press) pp 581–9